Available online at www.sciencedirect.com
ScienceDirect
Engineering Fracture Mechanics 74 (2007) 258–272
Engineering Fracture Mechanics
www.elsevier.com/locate/engfracmech

Effect of fiber reinforcement on the response of structural members

G. Fischer [a,*], Victor C. Li [b]

[a] Department of Civil Engineering, Technical University of Denmark, Building 118, DK-2800 Kgs. Lyngby, Denmark
[b] Department of Civil and Environmental Engineering, University of Michigan, GGB Building, Rm 2326, Ann Arbor, MI 48109-2125, USA

Available online 23 March 2006

Abstract

This paper describes a series of investigations on the effect of fiber reinforcement on the response of structural members in direct tension and flexure under reversed cyclic loading conditions. The design approach of the fiber reinforced cementitious composite is based on fracture mechanics principles, which will be described in the first part of the paper along with an introduction of the relevant material properties of the resulting engineered cementitious composite (ECC). This class of composites is characterized by strain hardening and multiple cracking properties in uniaxial tension and an ultimate tensile strain capacity on the order of several percent. Subsequently, the synergistic effects of composite deformation mechanisms in the ECC and structural members subjected to large shear reversals are identified. Beneficial effects observed in the reinforced ECC structural members as compared to conventional reinforced concrete include improved composite integrity, energy dissipation, ductility, and damage tolerance.

1. Tensile stress–strain characteristics of cementitious matrices

The deformation characteristics of cementitious matrices in tension are distinguished according to their postcracking deformation behavior [1]. Brittle matrices, such as plain mortar and concrete, lose their tensile load-carrying capacity almost immediately after formation of the first matrix crack (Fig. 1). The addition of fibers in conventional fiber reinforced concrete (FRC) can increase the toughness of cementitious matrices significantly, however, their tensile strength and especially strain capacity beyond first cracking are not enhanced. FRC is therefore considered to be a quasi-brittle material with tension softening deformation behavior (Fig. 1), i.e. a decaying load and immediate localization of composite deformation at first cracking in the FRC matrix.

* Corresponding author. Tel.: +45 45 25 5007; fax: +45 45 88 3282.
E-mail addresses: gf@byg.dtu.dk (G. Fischer), vcli@engin.umich.edu (V.C. Li).

0013-7944/$ - see front matter © 2006 Elsevier Ltd. All rights reserved.
doi:10.1016/j.engfracmech.2006.01.027

Nomenclature

σ_B	fiber bridging stress
$\sigma_{B,peak}$	maximum fiber bridging stress
σ_{fc}	composite first cracking strength
ε_o	composite strain at maximum compressive stress
δ_{peak}	crack opening at maximum bridging stress
δ_{ss}	steady-state crack opening
σ_{ss}	steady-state cracking stress
δU	elastic energy reduction
E	composite elastic modulus (uncracked)
f'_c	composite compressive strength
G_{tip}	matrix toughness
L	length of specimen
S_B	fiber bridging stiffness
V_f	fiber volume fraction
W_B	energy consumed by fiber stretching and pullout
W_m	energy consumed by matrix cracking
ΔL	deformation of specimen

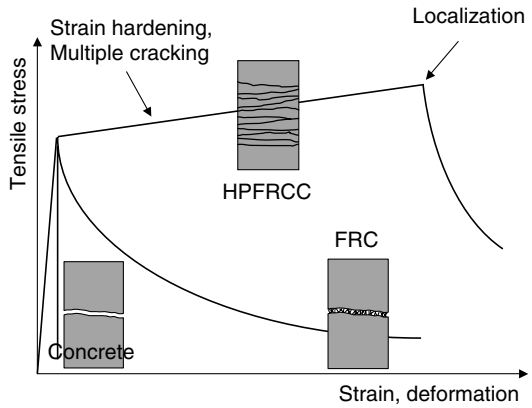

Fig. 1. Schematic stress–strain behavior of cementitious matrices in tension.

High performance fiber reinforced cement composites (HPFRCC) are defined by an ultimate strength higher than their first cracking strength and the formation of multiple cracking during the inelastic deformation process (Fig. 1) [1]. In contrast to localized deformation in conventional FRC, where the apparent strain is dependent on the gage length, the deformation of HPFRCC is uniform on a macro-scale and considered as pseudo-strain, which is a material property and independent of the gage length. The wording pseudo-strain hardening is used to distinguish the cracking-based deformation behavior in HPFRCC from strain-hardening in metals due to dislocation micromechanics. A particular version of HPFRCC, a micromechanically designed, engineered cementitious composite (ECC) [2] is used and elaborated on in the present study.

2. ECC design approach

The main feature of HPFRCC in general and ECC in particular is the formation of multiple cracking at increasing composite tensile stress. This behavior hinges on two complementary requirements, specifically

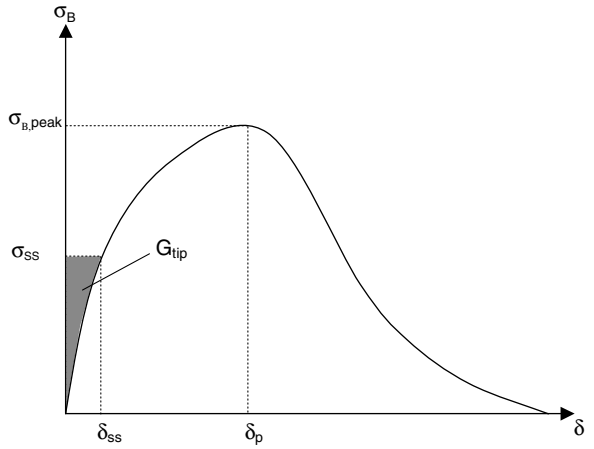

Fig. 2. σ_B–δ curve and parameters for composite strain hardening.

the peak bridging stress $\sigma_{B,peak}$ exerted by the fibers at the cracked section must exceed the first cracking strength of the matrix σ_{fc}, i.e.

$$\sigma_{B,peak} > \sigma_{fc}$$

such that the applied stress prior to matrix cracking can be carried by the fibers after matrix cracking. Furthermore, at formation of a matrix crack, propagation must occur at constant ambient stress σ_{ss} and constant crack opening δ_{ss} (Fig. 2) in order to achieve a uniform cross-sectional stress distribution [3]. The latter condition can be expressed as an energy balance between the external work, the energy necessary to propagate the matrix crack, and the energy dissipated by the bridging fibers, i.e.

$$\sigma_{ss}\delta_{ss} = G_{tip} + \int_0^{\delta_{ss}} \sigma_B(\delta)\,d\delta, \tag{1}$$

where G_{tip} is the matrix toughness and δ is the crack opening.

The combination of both conditions yields an upper limit for the matrix toughness G_{tip}

$$G_{tip} < \sigma_{B,peak}\delta_{peak} - \int_0^{\delta_{ss}} \sigma_B(\delta)\,d\delta. \tag{2}$$

The energy supplied at maximum fiber bridging stress $\sigma_{B,peak}$ and corresponding crack opening δ_{peak} reduced by the energy consumed in elastic fiber stretching and irreversible fiber pullout must be sufficient to accommodate a steady state crack propagation, i.e. must exceed the matrix toughness at the crack tip G_{tip}.

In order to satisfy these conditions, a large fiber volume fraction V_f can be employed, such as in SIFCON [4] and SIMCON [5], which require fiber contents $V_f > 5\%$ and show considerable postcracking tensile strength, however, limited tensile strain capacity prior to crack localization. In order to satisfy the above stated requirements at a minimum fiber volume fraction of a given fiber type in a given cementitious matrix, the properties of the cementitious matrix, the fiber, and the fiber/matrix interface must be considered. The micromechanical interaction of these constituents is the basis of design of engineered cementitious composites (ECC) as it affects the prerequisite mechanisms leading to steady state cracking and subsequent preservation of the composite load carrying capacity. Beyond formation of this particular type of crack, the characteristics of the stress–strain relationship of a given composite system are further governed by the bridging stress-crack opening relationship and the flaw size distribution in the cementitious matrix.

3. ECC stress–strain behavior in uniaxial tension

The composite tensile stress–strain behavior is outlined by the stress and strain at first cracking and at ultimate (Fig. 1). The specific characteristics, i.e. number and magnitude of stress fluctuations at crack formation

and rate of stress recovery, are influenced by the opening of an individual crack and spacing between multiple cracks at a given composite deformation state. The comparison of two particular types of ECC, specifically PE-ECC ($V_f = 1.5\%$) and PVA-ECC ($V_f = 2.0\%$) indicates similar composite ultimate strength and strain capacity, however, the detailed shape of their stress–strain curve differs considerably (Fig. 3). Both composites have individual mix proportions tailored to meet the required micromechanical conditions for tensile strain hardening and multiple crack formation.

The properties of the fiber and the fiber/matrix interface, characterized by the bridging stress/crack opening relationship (σ_B–δ curve), determine the opening of an individual crack at a given deformation state of the composite and subsequent temporary reduction in composite stress (Fig. 4). Prior to matrix cracking, the composite tensile stiffness E is essentially equal to the stiffness of the cementitious matrix and first cracking occurs when the ambient stress is sufficient to initiate propagation of cracking at the location of the largest matrix flaw (Fig. 5). The instantaneous stress drop at formation of a crack corresponds to a reduction in elastically stored energy δU in the composite, as indicated by the area OAA′ (Fig. 4) equal to the energy consumed by crack formation W_m in the cementitious matrix as well as the sum of energy W_B stored in elastic fiber stretching and consumed by fiber pullout (Fig. 5). Assuming similar matrix toughness G_{tip} in PE-ECC and PVA-ECC, the shape of the σ_B–δ curve (Fig. 5) largely influences the elastic energy reduction and magnitude of stress drop in the composite.

The magnitude of instantaneous stress reduction in the composite stress–strain curve is determined by the magnitude of internal strain redistribution due to elastic contraction of the uncracked segments and fiber stretching, i.e. crack opening δ_{eq} at equilibrium, and pullout at force equilibrium between ambient load and fiber bridging at fixed composite deformation (Fig. 6). This redistribution is directly influenced by the

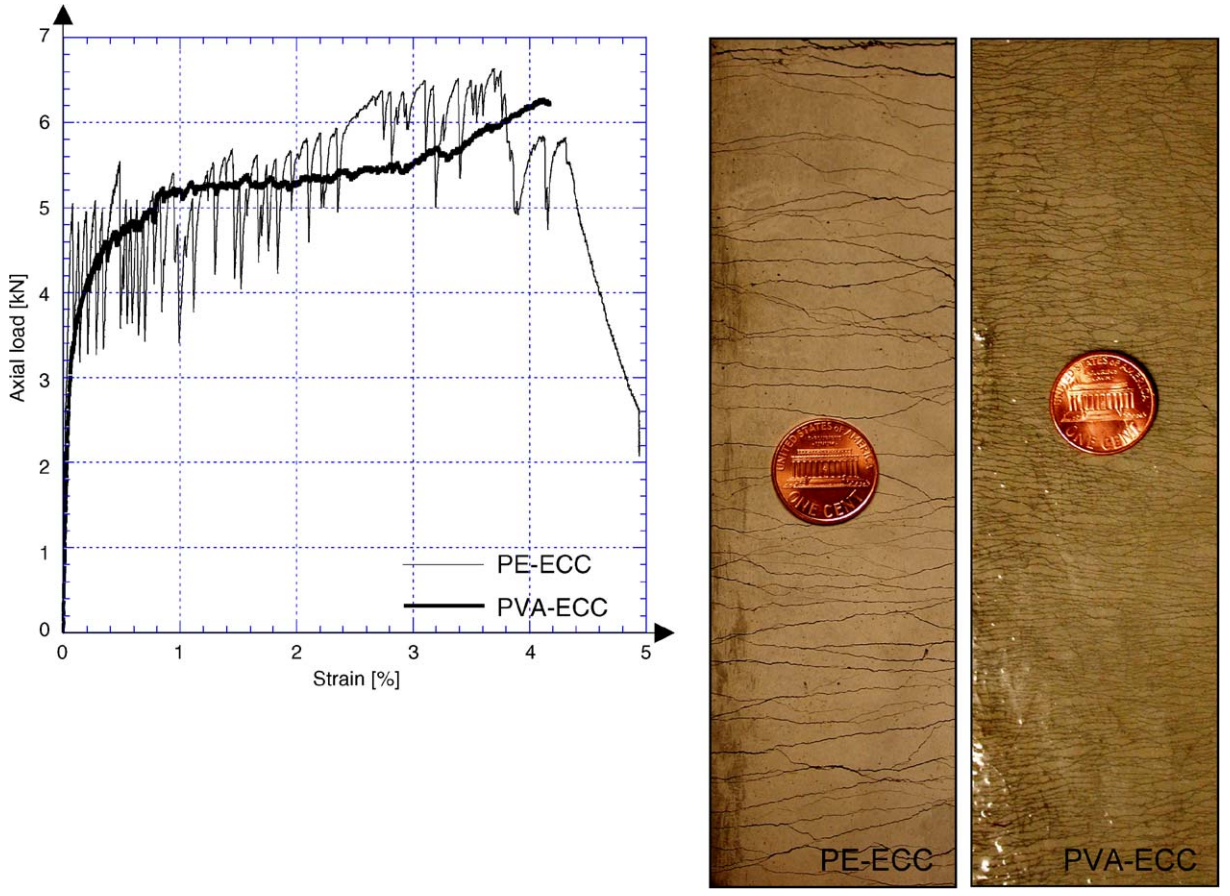

Fig. 3. Tensile stress–strain behavior of ECC and deformed shape of specimens.

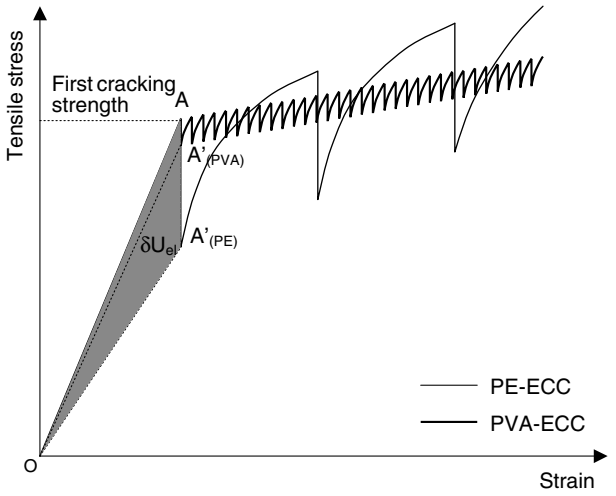

Fig. 4. Composite response at crack formation.

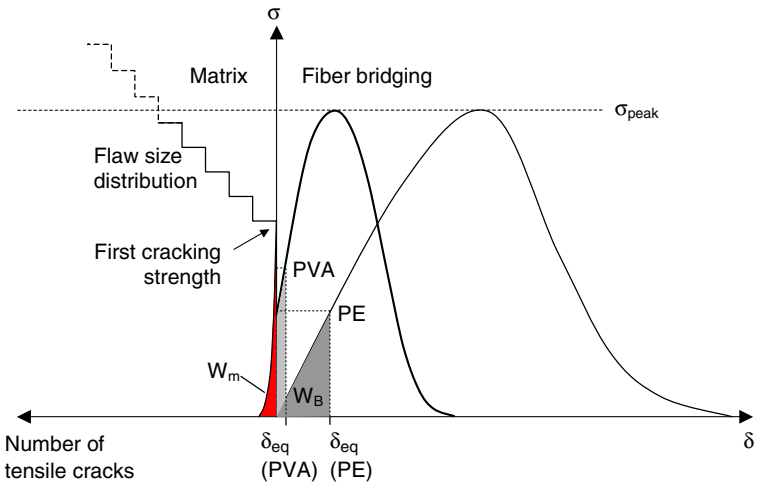

Fig. 5. Influence of constituents on composite crack formation.

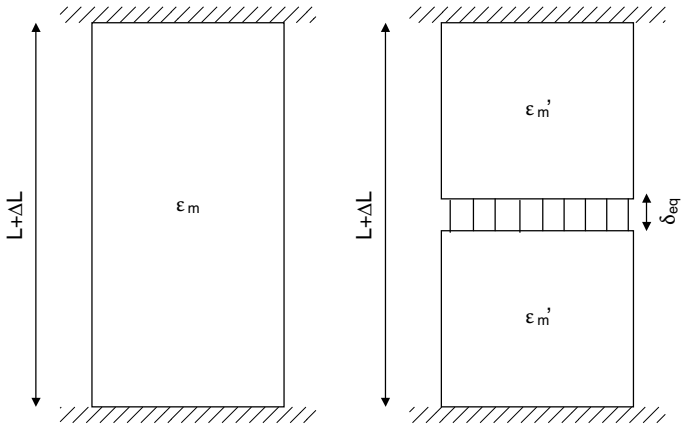

Fig. 6. Composite deformation before and after crack formation.

σ_B–δ curve, which for PVA-ECC shows an initial bridging stress at zero pullout length, corresponding to zero crack opening, and subsequently a relatively large bridging stiffness S_B at increasing crack opening. In contrast, the σ_B–δ curve of PE-ECC indicates zero initial bridging stress and relatively small bridging stiffness S_B at increasing crack opening. Depending on the crack opening δ_{eq} necessary to equilibrate the forces due to elastic contraction of the uncracked matrix, the stress drop is relatively large for PE-ECC and relatively small for PVA-ECC. Similarly, stress recovery and increase after matrix cracking, are further determined by the slope of the σ_B–δ curve, which results in relatively rapid stress increase in PVA-ECC and more gradual stress increase in PE-ECC in order to activate the second largest matrix flaw at increasing composite stress (Fig. 5). The shape of the σ_B–δ curve, particularly the initial bridging stiffness S_B, is influenced by the fiber volume fraction V_f, the elastic modulus of the fiber, and dominated by the interfacial bond properties of the fiber/matrix interface, which is significantly different due to the hydrophilic and hydrophobic nature of interfacial bond in PVA- and PE-ECC, respectively.

Consequently, stress transfer between fibers at the cracked section and adjacent cementitious matrix occurs over a relatively small fiber embedment length in PVA-ECC, which enables initiation of additional matrix cracking at relatively small crack spacing. Assuming similar flaw size distribution in PE-ECC and PVA-ECC, this results in a large number of stress fluctuations of small magnitude in PVA-ECC and conversely a relatively small number of stress fluctuations of large magnitude in PE-ECC (Figs. 3 and 4).

The deformed shape of the composite under direct tensile loading confirms these interaction mechanisms, where PE-ECC shows an average crack width of 200 μm at a spacing of approximately 4 mm whereas PVA-ECC shows a crack width of 25 μm at a spacing of 0.5 mm (Fig. 3).

Multiple crack formation stabilizes when all available matrix flaws at maximum fiber bridging stress have been activated and further increasing composite deformation is predominantly accommodated by increasing crack opening as opposed to further crack initiation. Failure of the composite occurs when the ambient stress exceeds the bridging strength of a particular cracked section where composite deformation localizes. Beyond this stage, the composite shows tension softening behavior similar to the post-peak behavior of conventional FRC (Fig. 1).

4. Parameters affecting the σ_B–δ curve

The σ_B–δ curve results from the load-crack opening response of the summation of all fibers bridging a crack, which can be at different stages of interface debonding and fiber pullout depending on their position and orientation relative to the crack plane at a given crack opening.

The extraction of an individual fiber from the surrounding matrix occurs in a sequence of interfacial debonding and subsequent fiber pullout. Interfacial debonding of a PE fiber is dominated by friction due to the hydrophobic nature of the fiber, while PVA fiber debonding is dominated by a strong chemical bond due to the hydrophilic nature of the fiber. This chemical bond is analogous to static friction whereas fiber pullout corresponds to kinetic friction.

In case of Polyethylene (PE) fibers, the single fiber pullout curve (Fig. 7) indicates exclusively kinetic friction, i.e. immediate sliding of the debonded section of the fiber until the entire embedded fiber length is debonded [6]. At constant interfacial friction, fiber pullout would occur at decreasing load corresponding to the decrease in contact area, however, scraping of the fiber surface increases the frictional resistance as the relative slip between fiber and surrounding matrix increases. Hence, beyond full debonding of the fiber, the applied load P continues to increase up to peak load and subsequently decreases until the fiber is completely pulled out. In order to fully utilize the tensile strength of the PE fiber and enhance the composite stress–strain behavior of PE-ECC, the interfacial bond strength is to be increased, e.g. by means of particular surface treatment [6].

In case of PVA fibers, chemical bonding requires a certain load to initiate fiber extraction (Fig. 7). Due to this dominant chemical bond, the fiber pullout load rapidly increases to a first peak in the P–δ curve and is followed by a sudden load drop as debonding unstably propagates to the fiber end. Subsequently, kinetic friction dominates the pullout process, accompanied by a strong increase in frictional resistance due to fiber surface scraping. This results in a gradual reduction of fiber diameter and ultimate rupture of the fiber.

In essence, PE fiber has a relatively low frictional strength and reaches its maximum pullout load at relatively large pullout length, while PVA fiber has a high frictional strength and reaches its peak load at relatively

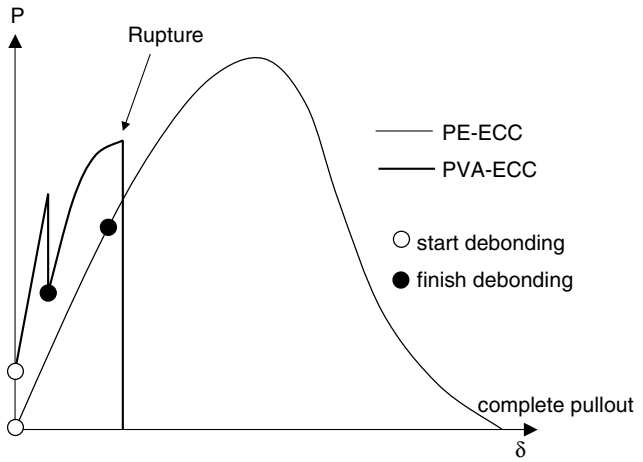

Fig. 7. Schematic of single fiber pullout response.

small pullout length, however, does not completely pullout of the matrix but ruptures in the extraction process. In order to increase the opening of an individual crack and enhance the composite stress–strain behavior of PVA-ECC, the static and frictional bond of the PVA fiber is to be decreased, e.g. by means of particular surface treatment [7] or by modification of the cementitious matrix by means of particle densification.

5. Composite stress–strain behavior in compression

The compressive stress–strain behavior of the cementitious matrices used in this study is defined by the elastic modulus E, the compressive strength f_c', and the strain ε_o at reaching the compressive strength. The experimentally determined stress–strain curves for PE-ECC and PVA-ECC are shown in Fig. 8.

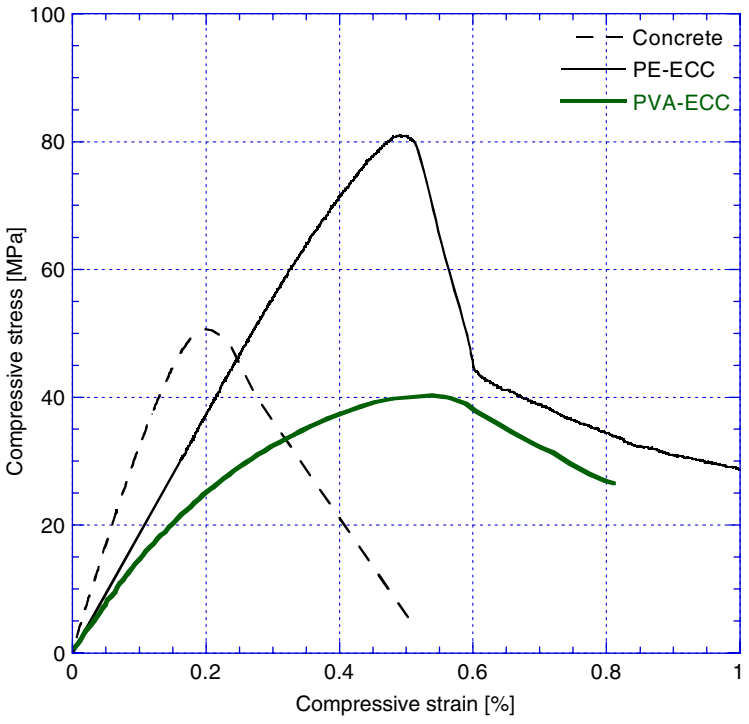

Fig. 8. Stress–strain behavior of cementitious matrices in compression.

PE-ECC shows a relatively high compressive strength compared to that of PVA-ECC due to the different aggregate size used in both composites. In PE-ECC, sand with a maximum diameter of 300 μm has been used, which satisfies the requirements on the matrix toughness G_{tip} and results in a relatively large composite elastic modulus at the given volume fraction. In order to satisfy the limits on the matrix toughness G_{tip} in PVA-ECC, sand particle size must be reduced or be replaced by limestone powder, which consequently leads to a relatively low composite elastic modulus in compression.

Similarly, the compressive strength of PE-ECC is larger than that of PVA-ECC, while both attain their respective peak stress at approximately 0.5% strain. Beyond reaching the compressive strength, PE-ECC shows a relatively rapid stress reduction to approximately 50% of the peak stress and subsequently a gradual stress reduction at further increasing compressive deformations. Because the peak stress in PVA-ECC is relatively low, the immediate stress drop beyond peak is insignificant, resulting in a rather ductile mode of failure. In contrast, concrete reaches its compressive strength at 0.2–0.3% strain and shows a relatively steep descending branch in post-peak deformation regime.

In addition to the inelastic strain capacity of ECC in tension, the differences in compressive stress–strain characteristics between ECC and concrete are expected to have a significant influence on the flexural behavior of reinforced ECC and concrete members particularly in the inelastic deformation regime.

6. Interaction of ECC and steel reinforcement

Due to the particular material properties of ECC, a steel reinforced ECC member can be considered as a combination of a ductile cementitious matrix (ECC) and a reinforcing ductile element (steel). Evidence to support this approach can be obtained by investigating the deformation behavior of a steel reinforced ECC (R/ECC) member in uniaxial tension in contrast to that of conventional steel reinforced concrete (R/C).

The contribution of the cementitious matrix to the load–deformation response of reinforced concrete or ECC in uniaxial tension is generally described as tension-stiffening effect. The response of the reinforced cement composite is compared to that of the bare steel reinforcement and the difference is attributed to the tensile load carried by the cementitious matrix between transverse cracks.

Schematically, the difference in tensile load–deformation response between R/C and R/ECC can be described using a representative composite element (Fig. 9). Prior to reaching the first cracking strength of the cementitious matrix, the applied composite load is shared between reinforcement and matrix proportional

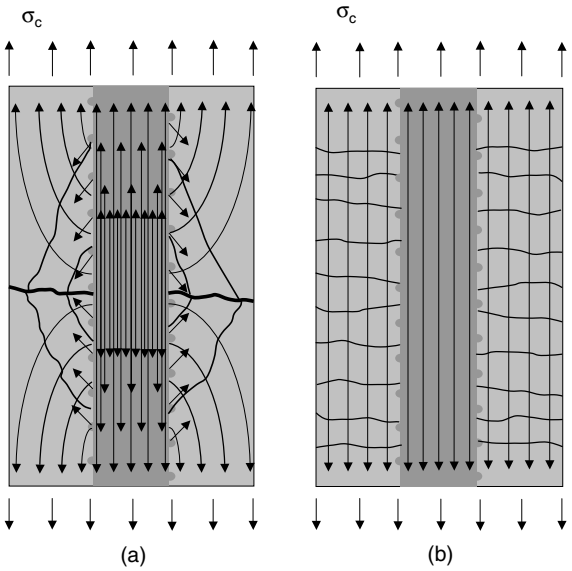

Fig. 9. Crack formation and internal stresses in R/C and R/ECC composite: (a) R/C after matrix cracking, (b) R/ECC after matrix cracking.

to their stiffness and volume fraction. Stresses in both components are uniformly distributed in sections beyond the load transfer zone of the specimen. The formation of a transverse crack in the R/C composite causes a redistribution of stresses in the matrix as well as in the reinforcement (Fig. 9a). Since the concrete matrix is not able to transfer load across the crack, the applied load must be transferred to the reinforcement by bond action and is entirely carried by the reinforcement at the crack location. Due to the stress concentration in the reinforcement and the stress-free concrete matrix at the crack location, both materials experience a relatively large strain difference resulting in bond stresses and local slip. Consequently, composite deterioration can occur in various scenarios, such as interfacial bond failure, formation of inclined cracks originating from the interface, and longitudinal splitting due to radial pressure exerted by the ribs of the deformed reinforcing bar on the surrounding concrete.

The tensile ductility of the ECC matrix can on a macro scale eliminate the strain difference between reinforcement and matrix material. The R/ECC member may be considered as a composite of two materials having elastic/plastic deformation behavior with individual yield strength and strain. As a result of these similar deformation characteristics, both constituents of the R/ECC composite are deforming compatibly in the elastic and inelastic deformation regime.

Cracking of ECC represents yielding of the matrix component while the steel reinforcement remains elastic. After cracking the stress distribution in the R/ECC composite is virtually unchanged (Fig. 9b) since the stress in the ECC matrix at this instance remains constant and further increases with increasing deformation. In essence, the tensile load carried by the matrix prior to cracking is directly transferred (via bridging fibers) to the uncracked parts of the matrix once the crack has formed. On a macro scale, bond stresses are not required to facilitate this transfer since load carried by the ECC matrix need not be transferred to the reinforcement. Due to the uniform stress in the cracked matrix, the distance between transverse cracks is a function of material properties of the fiber reinforced cement composite (ECC) and is independent of the interfacial bond properties between reinforcement and matrix. However, considering local effects in the immediate vicinity of one discrete crack in the ECC matrix, some interaction between reinforcement and matrix is expected. Depending on the micromechanical properties of the ECC matrix, a certain crack opening is required to develop a fiber bridging stress equal to that of the composite prior to cracking. Due to this microscopic discontinuity, localized interfacial bond between steel reinforcement and ECC matrix is activated.

Yielding of the steel component constitutes the final deformation stage of the R/ECC member, where both constituent materials have entered the inelastic deformation regime. Strain-hardening deformation behavior of both components (steel and ECC) prevents localization of deformation at a particular section and compatible inelastic deformations of steel and ECC are maintained. Cracking of ECC as well as yielding of reinforcement is uniformly distributed over the length of the specimen. Because of the large volume of material involved in the inelastic deformation process, energy absorption is significantly enhanced. The fact that the ECC contribution to the load-carrying capacity can be maintained at relatively large deformation levels beyond steel yielding is directly attributed to the ductility of the ECC matrix, i.e. its multiple cracking deformation behavior.

These mechanisms in R/ECC composites have been experimentally verified and contrasted to the tension stiffening behavior of R/C composites. The comparison of the load–deformation response of R/ECC and R/C subjected to uniaxial tensile deformations clearly indicates the contribution of the ECC matrix to the load-carrying capacity particularly in the post-cracking and post-yielding regime (Fig. 10).

Furthermore, the assumption of compatible deformations between ECC and steel reinforcement at large inelastic deformations is verified by observations on the interface between reinforcement and cementitious matrix after termination of the test. In the R/C specimen, the interface between concrete and steel in the vicinity of the transverse crack is debonded and inclined cracking in the concrete matrix indicates the inability of concrete to accommodate the deformations induced by the steel reinforcement beyond yielding (Fig. 11). In the R/ECC specimen, simultaneous yielding of steel and multiple cracking of ECC prevent the activation of significant interfacial bond stress and consequently, the interface between steel reinforcement and ECC matrix remains intact throughout the elastic and inelastic deformation process of the R/ECC composite (Fig. 11). Further details of this experimental investigation on the tension stiffening effect of ECC can be found in [8].

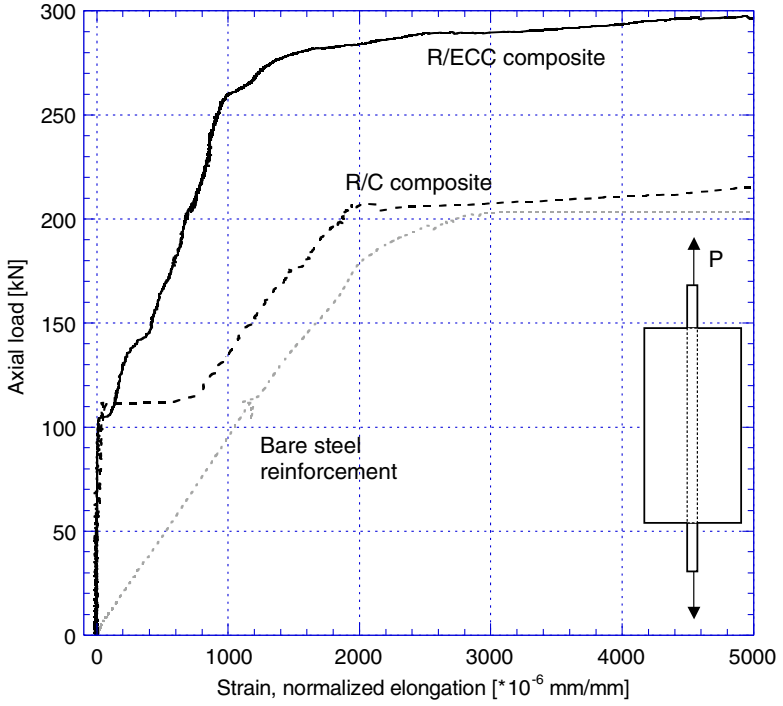

Fig. 10. Axial load–deformation response of R/C and R/ECC.

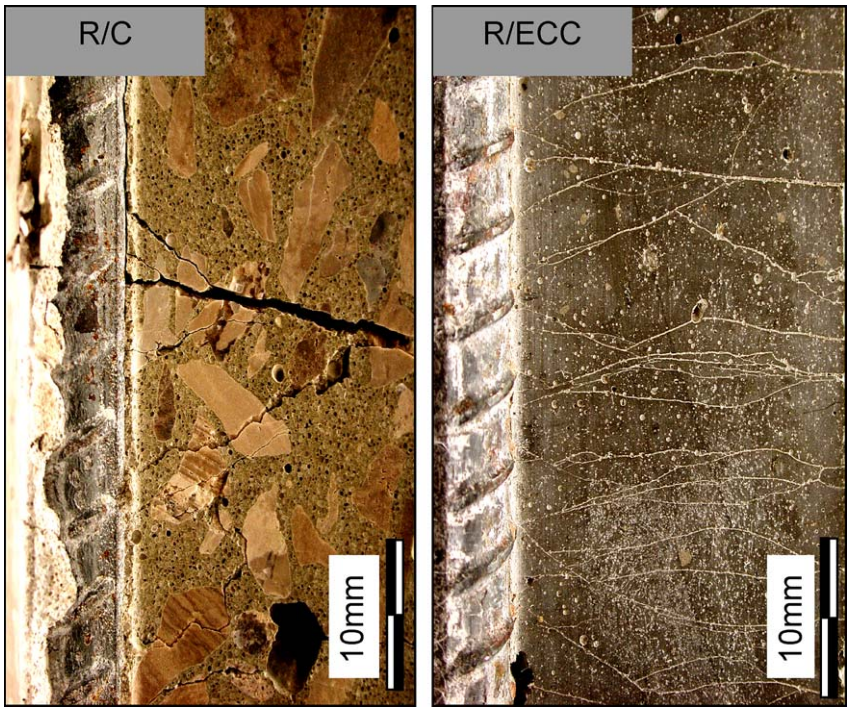

Fig. 11. Interface condition beyond yielding of steel reinforcement in R/C and R/ECC.

7. Flexural deformation behavior of steel reinforced ECC members

The preservation of composite integrity at relatively large deformations through the mechanisms described above for uniaxial tension has advantageous effects on the behavior of reinforced ECC flexural members especially under reversed cyclic loading conditions. Compatible deformation of ECC and longitudinal reinforcement will directly enhance the tensile component and indirectly ensure stable inelastic deformation on the compression side of the flexural member.

The performance of structures required to resist seismic excitations is dependent on the ability of selected structural components, in particular flexural members such as beams and columns in a moment resisting frame, to sustain relatively large inelastic deformations without significant loss of load carrying capacity. The ductility of these typical reinforced concrete components is indirectly dependent on the amount and configuration of transverse steel reinforcement, which serves as confinement of the concrete core and shear capacity enhancement and also provides resistance against buckling of longitudinal reinforcement.

Particularly under reversed cyclic loading conditions, the fundamental source of damage observed in reinforced concrete structures is the brittleness of concrete in general but in tension in particular. Structural deficiencies associated with this material property, such as bond splitting, concrete spalling, flexural strength decay due to shear failure, brittle compression failure and buckling of longitudinal reinforcement are usually overcome by arranging transverse reinforcement in order to confine concrete in compression or divert internal tensile forces from concrete to the transverse reinforcement to resist shear and prevent buckling of longitudinal reinforcement. Transverse reinforcement can be considered an external means to counteract internal material deficiencies of concrete to achieve a virtually ductile deformation behavior in tension and compression, with an increasing amount of transverse reinforcement resulting in increased structural ductility. Consequently, critical locations of structural elements, such as plastic hinge regions and joints, can be heavily congested and difficulties may arise in arranging the required amount of transverse reinforcement and in proper placement of concrete in these congested zones.

Despite enhanced resistance to undesirable failure modes by providing transverse reinforcement, the inherently brittle deformation behavior of concrete cannot be modified and deficiencies with respect to steel/concrete interaction, interfacial bond deterioration, and composite integrity are not overcome. While properly designed reinforced concrete structures ensure sufficient resistance to seismic excitations and satisfy primary safety requirements, research activities presented herein are motivated by the need to improve secondary performance requirements, such as reinforcement detailing requirements (potential reinforcement congestion and concrete compactability), construction feasibility and quality, damage tolerance, and repair needs, which are of significant economical concern.

The inelastic response of R/ECC members under flexural load reversals is determined by the composite behavior in tension and compression, member shear resistance, matrix confinement effect, and resistance against buckling of longitudinal steel reinforcement. Considering the material properties of ECC and previous findings on the deformation mechanisms of R/ECC in tension, the inelastic flexural response can be described by two conceptual stages before and after transition from multiple cracking to localization of cracking. The description of these stages will focus on the inelastic response of R/ECC, however, prior to yielding of steel reinforcement, the ductile deformation behavior of ECC will also affect the flexural member response by a more uniform distribution of flexural cracking with reduced crack spacing and individual crack widths compared to reinforced concrete composites.

Beyond yielding of steel reinforcement and prior to localization of cracking in the ECC matrix, a given displacement of the R/ECC flexural member is expected to require a reduced peak curvature in the plastic hinge region compared to the R/C composite, resulting in reduced sectional demand on reinforcement tensile strain and compressive stress in ECC. This reduction of peak curvature is related to an extended distribution of deformation along the flexural member in particular beyond yielding of the longitudinal reinforcement (Fig. 12). Similar to the composite deformation mechanism in uniaxial tension, the distribution of deformation is due to simultaneous strain-hardening of ECC and steel reinforcement. Besides reduced sectional demand, interfacial bond stresses are negligible due to compatible deformation between reinforcement and ECC and radial bond splitting forces are not generated. Consequently, longitudinal bond splitting cracks will not occur, which is expected to prevent interfacial bond deterioration, cover spalling and composite disintegration under

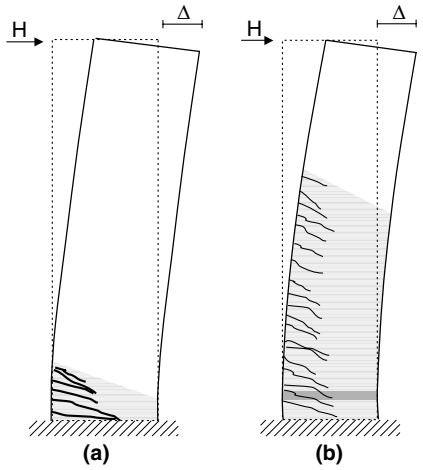

Fig. 12. Idealized flexural deformation behavior of (a) R/C and (b) R/ECC.

tension and compression alternations. Thus, prior to localization of matrix cracking, the R/ECC member essentially benefits from a reduced sectional demand due to distributed flexural deformation along the specimen as opposed to localized crack formation observed in conventional R/C members (Fig. 12).

In the second stage, the strain capacity of ECC at the cantilever base is exhausted at a certain deflection level and localization of cracking leads to a concentration of deformation at this section. At this stage, the sectional demand is similar to that of reinforced concrete and consequently, deformation compatibility is lost and interfacial bond stresses are initiated. Slip between steel reinforcement and ECC causes radial stresses in the cementitious matrix, which in R/C members lead to bond splitting and spalling of the concrete cover. In R/ECC, bond splitting cracks may occur beyond localization of flexural cracking in ECC, however, in the transverse direction ECC remains in the strain-hardening regime with continuing resistance against cover spalling and reinforcement buckling. At this deformation stage, the R/ECC member benefits from the tensile strength of ECC beyond cracking, more specifically its confining effect and resistance against cover spalling.

Throughout both deformation stages, ECC is found to resist premature failure modes. Due to the intrinsic shear strength of ECC, additional transverse reinforcement provided by stirrups in potential plastic hinge regions and beyond may be significantly reduced. Moreover, the confinement effect of the ECC cover provides lateral resistance against buckling of steel reinforcement in the form of a continuous embedment similar to the effect of a confining jacket, which is additionally anchored into the ECC core by means of fiber bridging. The same mechanism also actively confines the ECC core, resulting in a ductile failure mode in compression.

With respect to structural ductility, the most important contribution of ECC to the structural response of the member is to maintain composite integrity and provide lateral stability for the reinforcing steel in order to endure cyclic inelastic deformations without buckling. Despite its considerable ductility in uniaxial tension, the cyclic behavior of ECC differs from that of a ductile metal, in that ECC is unable to recover its energy dissipation mechanism under alternating inelastic tensile and compressive deformations. Therefore, direct contributions of ECC to member flexural strength and energy dissipation are expected to be relatively small. However, its stabilizing effect on the longitudinal steel reinforcement and damage tolerance at large deformations are expected to considerably improve structural performance with respect to member energy dissipation capacity and damage evolution.

The load–deformation response of steel reinforced ECC members has been experimentally investigated and contrasted to a conventional R/C member (Fig. 13). The geometry, longitudinal reinforcement and loading configuration are identical in both specimens, while transverse steel reinforcement is provided in the R/C specimen only. The comparison indicates performance improvements resulting from the ductile deformation behavior of ECC. In particular, the energy dissipation capacity of R/ECC is significantly enhanced. The intrinsic shear capacity of ECC provides sufficient shear resistance for the reinforced member. Additional

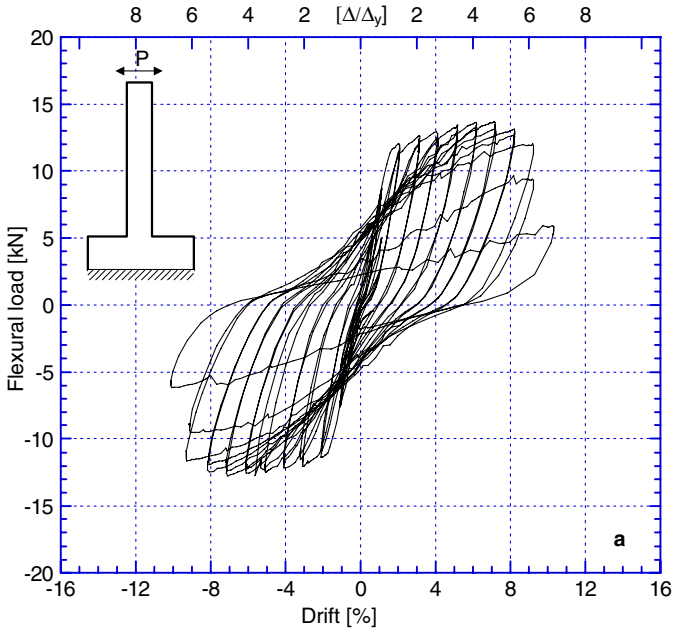

Fig. 13a. Load–deformation response of the R/C cantilever specimen with steel reinforcement.

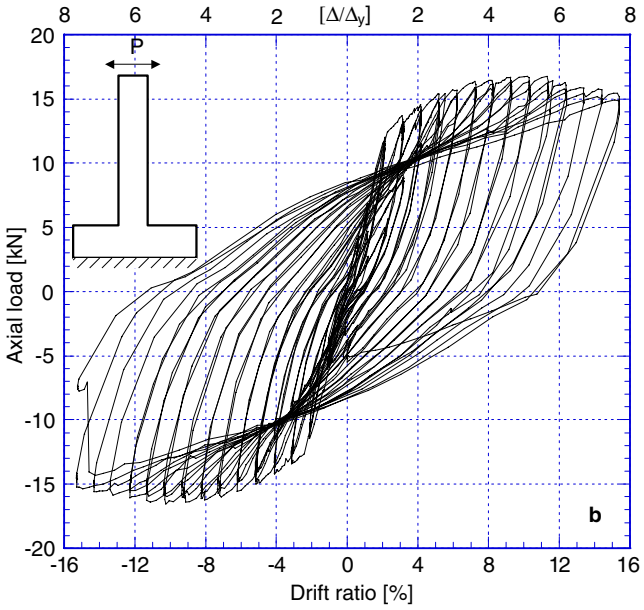

Fig. 13b. Load–deformation response of the R/ECC cantilever specimen with steel reinforcement.

transverse steel reinforcement is ineffective and redundant in R/ECC flexural members at given aspect ratio and low axial load levels.

Damage in R/ECC members is dominated by flexural cracking of ECC and stable inelastic deformations of steel reinforcement. ECC shows considerably higher damage tolerance than confined concrete. Bond splitting and spalling of ECC as well as composite disintegration due to cyclic loading are prevented (Fig. 14). Further details of the investigation on the effect of ECC on the flexural deformation behavior of structural members under reversed cyclic loading can be found in [9].

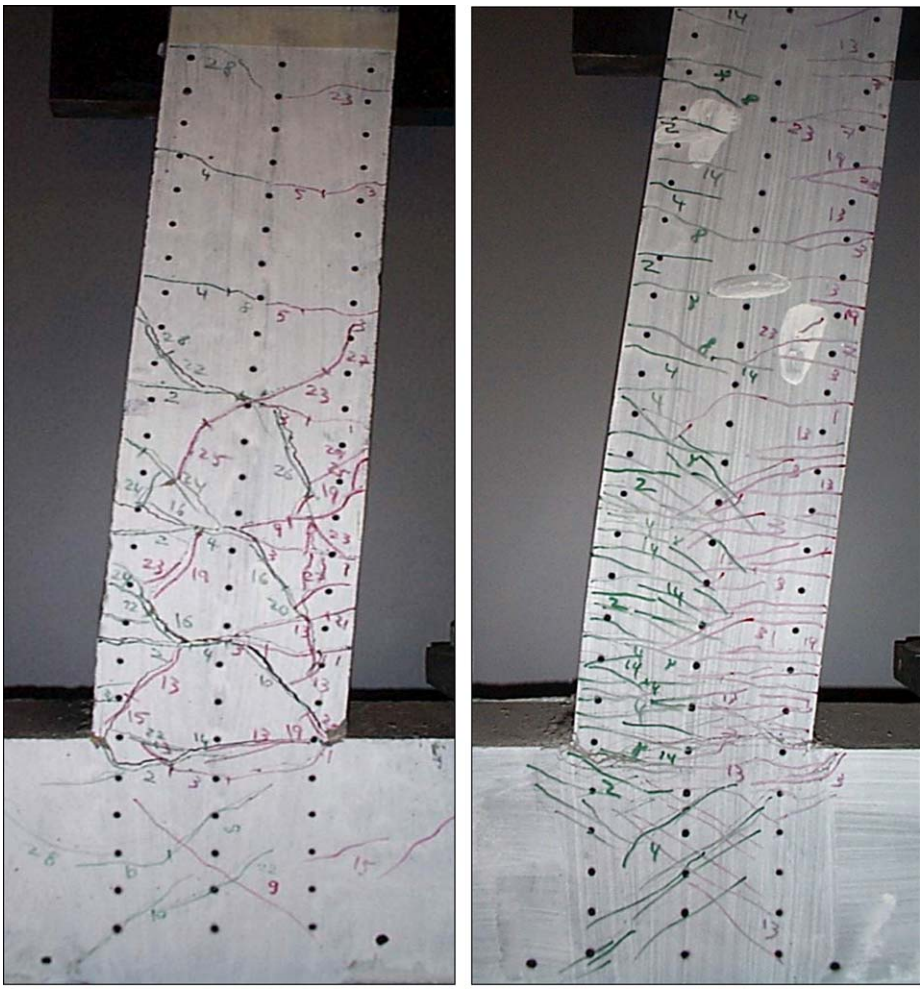

Fig. 14. Deformed shape of (a) R/C specimen and (b) R/ECC specimen at respective peak load.

8. Conclusions

The effects of fiber reinforcement on the material properties of ECC, in particular the tensile stress–strain response and associated deformation characteristics, have been identified and experimentally demonstrated. The transition from ECC material properties to the behavior of structural members utilizing this material is fundamentally governed by the interaction of ECC and structural steel reinforcement in tension. Their similar elastic/plastic material properties lead to compatible deformations of both components in the elastic and inelastic deformation regime. Consequently, damage induced by local slip and excessive interfacial bond stress between steel reinforcement and cementitious matrix is prevented, resulting in improved performance of the reinforced ECC element in terms of axial loading capacity, ductility, and composite integrity. These synergistic effects are not primarily achieved by increased resistance of the materials in terms of tensile strength, confinement effect, or interfacial bond strength, but rather by reduced internal stresses and higher tolerance to damage typically observed in reinforced concrete structural members.

The material properties of ECC, in particular the ductility, affect the tension stiffening effect of the cementitious composite. It is found that multiple cracking has a significant impact on the structural response resulting in compatible deformations between steel reinforcement and ECC in the inelastic deformation regime. While a considerable tension stiffening and strengthening effect is found in monotonic uniaxial tension, the

contribution of ECC to the flexural strength of the reinforced structural member under cyclic loading conditions is found insignificant. Similarly, the extreme ductility of ECC is found to have no substantial direct contribution to the structural ductility, however, indirectly enhances the ductility of the member significantly.

For structural applications where concrete is substituted with ECC in particular or with FRCC in general, inelastic deformation capacity and damage tolerance rather than strength of the fiber reinforced cementitious composite are of paramount importance and should guide the composite design for structural performance. The addition of fiber reinforcement itself cannot be directly correlated to structural performance, but rather the material properties of ECC should be used to integrate materials design on the micro-scale with structural design on the macro-scale.

References

[1] Naaman AE, Reinhardt HW. Characterization of high performance fiber reinforced cement composites-HPFRCC. In: Naaman AE, Reinhardt HW, editors. Proceedings of high performance fiber reinforced cement composites 2 (HPFRCC 2), 1995, pp. 1–23.
[2] Li VC. Engineered cementitious composites – tailored composites through micromechanical modeling. In: Banthia N, Bentur A, Mufti A, editors. Fiber reinforced concrete: present and the future. Montreal: Canadian Society for Civil Engineering; 1998. p. 64–97.
[3] Li VC, Leung CKY. Steady-state and multiple cracking of short random fiber composites. J Engng Mech, ASCE 1992;118(11): 2246–63.
[4] Naaman AE. SIFCON: Tailored properties for structural performance. In: High performance fiber reinforced cement composites, E&F Spon, 1992, pp. 18–38.
[5] Krstulovic-Opara N, Malak S. Tensile behavior of slurry infiltrated Mat Concrete (SIMCON). ACI Mater J 1997(January–February): 39–46.
[6] Li VC, Wu HC, Chan YW. Effect of Plasma Treatment of Polyethylene Fibers on Interface and Cementitious Composite Properties. J Am Ceram Soc 1996;79(3):700–4.
[7] Li VC, Wu C, Wang S, Ogawa A, Saito T. Interface Tailoring for Strain-hardening PVA-ECC. ACI Mater J 2002;99(5):463–72.
[8] Fischer G, Li VC. Influence of matrix ductility on the tension-stiffening behavior of steel reinforced Engineered Cementitious Composites (ECC). ACI Struct J 2002;99(1):104–11.
[9] Fischer G, Li VC. Effect of matrix ductility on deformation behavior of steel reinforced ECC flexural members under reversed cyclic loading conditions. ACI Struct J 2002;99(6):781–90.